Silicon chemical vapor deposition on macro and submicron powders in a fluidized bed

Loic Cadoret, Nicolas Reuge, Sreekanth Pannala, Madhava Syamlal, Cécile Rossignol, Jeannette Dexpert-Ghys, Carole Coufort, Brigitte Caussat

SILICON CHEMICAL VAPOR DEPOSITION ON MACRO AND SUBMICRON POWDERS IN A FLUIDIZED BED

Loïc CADORET[1], Nicolas REUGE[1], Sreekanth PANNALA[2], Madhava SYAMLAL[3], C. ROSSIGNOL[4], J. DEXPERT-GHYS[4], Carole COUFORT[1], Brigitte CAUSSAT[1]

[1]*Laboratoire de Génie Chimique, UMR CNRS 5503, ENSIACET/INPT, 5 rue Paulin Talabot, BP 1301, 31106 Toulouse Cedex 1, FRANCE*
Contact: Brigitte.Caussat@ensiacet.fr
[2]*Oak Ridge National Laboratory, Computational Mathematics Group, Bldg. 6012, MS-6367, RM-101, Oak Ridge, TN 37831, USA*
Contact: pannalas@ornl.gov
[3] *National Energy Technology Laboratory,* 3610 Collins Ferry Road, P.O. Box 880, Morgantown, WV 26507-0880*, USA*
Contact : Madhava.Syamlal@NETL.DOE.GOV
[4]*CEMES, UPR CNRS 8011, 29 rue Jeanne Marvig, 31055 Toulouse Cedex 4, FRANCE*
Contact: jdexpert@cemes.fr

Abstract. Titanium oxide (TiO_2) submicron powders have been treated by Chemical Vapor Deposition (CVD) in a vibro fluidized bed in order to deposit silicon layers of nanometer scale on each individual grain from silane (SiH_4). Experimental results show that for the conditions tested, the original granular structure of the powders is preserved for 90% of the initial bed weight while the remaining 10% consisted of agglomerates in millimetre range found near the grid of the reactor. A comparison between experimental and modelling results using the MFIX code shows that for Geldart's group B alumina particles (Al_2O_3), the model represents both the bed hydrodynamics and silane conversion rates quite well. The future objective is to extend the simulation capability to cohesive submicron powders in order to achieve better predictability of the phenomena governing ultrafine particles.

Keywords. Fluidized Bed; Chemical Vapor Deposition (CVD); Submicron powders; Silicon; Process modelling.

INTRODUCTION

The Fluidized Bed Chemical Vapor Deposition (FBCVD) process represents one of the most efficient ways to modify the surface properties of micro- or nano-powders. The most important applications concern the coating of powders against corrosion and oxidation or the synthesis of supported catalysts.

When coating powders using FBCVD, one major consideration is the fluidizability of the particles. Micronic powders belonging to Geldart's group C [1] are difficult to fluidize because the interparticle cohesive forces are often much greater than the drag force exerted by the fluid. Consequently when subjected to fluidization, they tend to agglomerate. These agglomerates have a dynamic behaviour: Hakim *et al.* [2] showed that the agglomerates form, break and reform and their size (up to 500 µm) and shape change with time.

To overcome this problem, activation of the fluidization process becomes necessary. Some authors ([3]-[5]) propose to improve fluidization by using mechanical stirrers inside the bed or introducing a small amount of large particles into the fine powders. More recently, Alavi & Caussat [6] and Xu & Zhu [7] showed that mechanical vibration increases the forces acting on particles and tend to break up agglomerates: both the average size and the segregation of agglomerates in the bed are thus reduced.

Due to its high complexity, the understanding and the prediction of fluidized bed (FB) dynamics is essential to design an optimal fluidization and coating strategy. Due to the rapid advances in computational capabilities, computational fluid dynamics (CFD) appears to be a promising tool. Due to the complex behaviour of gas-solid systems, the development of such multiphase flow simulation tools are still on going. For example, there is still no general agreement on the appropriate closure models [8], and terms such as the solid phase stresses or the interphase momentum transfer are still in the research and development phase.

Most of the works on simulation of gas-solids FB were carried out with particles of Geldart's group B ([9], [10], [11]). Due to the cohesive behaviour of Geldart's group C powders, the incorporation of cohesion into continuum models seems to have been rarely attempted [12]. Thus to correctly reproduce a cohesive FB, Weber [13] proposed to use a Lagrangian representation in which the interparticle forces are considered via a square-well or Hamaker model.

The implementation of kinetic models of CVD coupled with CFD codes also represents a challenging task. Indeed, chemistry is an essential part in calculations of reactive flows due to the wide range of length and time scales. The first step usually consists of establishing the grid independence to be sure that the bed hydrodynamics is accurately predicted before the reaction kinetics scheme can be implemented. At the present time, only Guenther *et al.* [14] simulated the dynamics of silicon CVD on a FB of group B alumina particles.

The present work deals with silicon FBCVD on macro and submicron powders. The first part goes into the study of silicon deposition on group C powders (TiO_2 particles) in a vibrated fluidized bed. The objective is to form nanometer scale continuous layers around each individual grain and thus preserve the original size distribution. In the second part, we present results about silicon deposition on macro powders of non porous alumina Al_2O_3. These experimental results form a data base for the simulation of the FB hydrodynamics coupled with the CVD process. Numerical results such as the height of the bed and the conversion rate of silane are compared with the experimental data.

EXPERIMENTAL

Figure 1 illustrates the experimental setup. The cylindrical column was made of stainless steel with an internal diameter of 0.05 m and a height of 1 m. The reactor was externally heated by a three-zone electrical furnace and the wall temperatures were monitored by three thermocouples. Several thermocouples were also placed into a tube of 6 mm in diameter inside the reactor as shown in Figure 1. An Inconel™ porous plate is used for the gas distribution. Silane and nitrogen were supplied to the bottom of the bed through ball rotameters associated to manometers. A differential fast response pressure sensor measured the total pressure drop across the bed; the high pressure tap was placed under the distributor and the other one was situated at the top of the column. The vibrated fluidization experiments were performed by fixing the reactor on a vibrating table as shown on Figure 1. Two vibro-motors were thus mounted on the opposite sides of the table to achieve the horizontal vibration of the column. Vibration frequency could be varied from 15 to 50 Hz and the vibration amplitude from 0.5 to 6 mm. An accelerometer measured the forces applied to the column by the vibration. A hydrogen detector (catharometer) provided the hydrogen concentration of the outlet effluents. A DasyLab® system enabled the on-line acquisition of the differential pressure, FB temperatures and H_2 outlet concentration. Some hydrodynamic measurements were performed in a glass transparent column of similar features using a video camera (Panasonic Tri CCD NV-GS400).

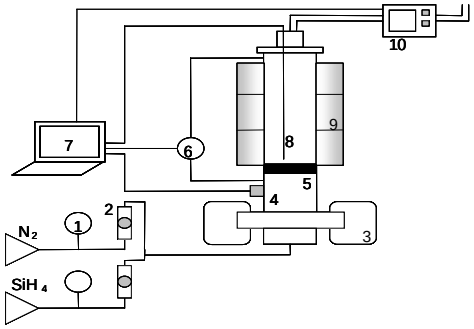

1. Manometer
2. Ball flowmeter
3. Vibro-motors
4. Accelerometer
5. Distributor
6. Pressure sensor
7. Data acquisition
8. Thermocouples
9. Furnace
10. Catharometer

Figure 1: Experimental set up.

Alumina (Al_2O_3) particles of Geldart's group B and titanium dioxide (TiO_2) group C powder were used in this study. Their main characteristics are summarized in Table 1. The cohesivity (C) and the Hausner Ratio (HR) of the Geldart's group C particles indicate that these powders are not fluidizable [15]; indeed we have verified that they form channels and slugs when fluidized resulting in a very poor gas-solids contact.

	$d_{0,5}$ (µm)	$d_{3/2}$ (µm)	Grain density (kg/m^3)	Geldart's group	HR (-)	C (%)	Form
Al_2O_3	342	329	3900	B	1.14	12.5	Broken solids
TiO_2	0.49	0.48	4000	C	1.75	43	Sphere

Table1: Characteristics of the different powders studied

Concerning CVD experiments, a theoretical thickness was deduced from the deposited silicon mass assuming that the particles were spherical and the deposition was uniform. The conversion rate of silane was deduced from the deposited mass and the hydrogen concentration at the outlet. The initial and final size distributions of the powders were measured by laser granulometer (MasterSizer2000). The deposition morphology was analysed by scanning electron microscopy (SEM) (LEO 435 VP). Some Raman spectroscopy measurements have been performed at the "Service de Spectroscopies Vibrationnelles" of the Paul Sabatier University (Toulouse) on a Labram HR800 from Jobin Yvon equipped with a laser He/Ne (ex: 632.8 nm). Some transmission electron microscopy (TEM), Infra Red (IR) spectroscopy and X Ray Diffraction (XRD) analyses have been performed respectively on a Philips CM20, a spectrometer (Perkin Elmer Series 100) and on a diffractometer (SEIFERT 3000TT) at CEMES.

VIBRO-FB CVD OF SILICON ON TIO_2 POWDERS OF 0.5 MICRON

Before beginning the first CVD experiments, a hydrodynamic study has been performed to identify the fluidization conditions (amplitude, frequency, total gas flow rate) that provide the best gas-solid contact. We found that fluidization was improved for a certain range of vibration intensities. But the bed always fluidized under the form of dynamic agglomerates and not as ''single'' particles. Without vibration, segregation took place in the bed: stagnant agglomerates with an approximate diameter of 2 mm were present near the distributor whereas smaller ones were observed at the top part of the bed (600 – 700 µm). We selected optimal conditions of vibration and gas flow rate involving minimal agglomerate size and maximal interphase contact all along the bed. In these optimal vibration conditions, segregation was much less significant with a mean agglomerate size varying from 300 µm at the top to 600 µm at the bottom of the bed. The influences of the distributor porosity, bed initial weight, gas velocity and direction of vibration were also examined. The qualitative results obtained were in good agreement with literature data [7]. These hydrodynamic results allowed us to perform first experiments of vibro FBCVD on TiO_2 powders as detailed in Table 2. The objective was to form nanometer scale continuous layers of silicon around each individual grain and to avoid particles agglomeration due to CVD. We have then chosen to work in a high chemical reactivity regime, i.e. with low inlet percentages of silane in nitrogen and at relatively low temperatures. The initial weight of powders was always 450 g corresponding to a ratio between the initial fixed bed height and the reactor diameter H_0/D close to 5.

Run	Temperatures (℃)		Weight of injected Si (g)	Run duration (min)	Calculated thickness of Si deposition (nm)
	Distributor	Top of the bed			
T1	550	605	3.7	72	1.4
T2	550	610	7.8	61	3.9
T3	550	610	3.8	72	1.4
T4	560	600	1.4	63	0.5
T5	505	585	1.7	64	0.6
T6	565	600	2.7	116	1
T7	560	610	31	60	15

Table 2: Operating conditions and experimental results for silicon deposition on TiO_2 powders

Due to the small SiH_4 inlet concentration and to the large specific surface area of powders, the silane conversion rate was always 100%. Then it is well known that silane SiH_4 begins to decompose around 370℃ [16]. As a consequence, it is mandatory to cool the zone below the grid to avoid its plugging by undesirable silicon deposition. This cooling is responsible for significant thermal gradients along the FB (from 40℃ to 80℃) as detailed in Table 2. Such gradients have already been mentioned in previous studies ([16], [17]). They are not too detrimental to the deposition uniformity as the particles are circulated axially inside the bed. During experiments, no de-fluidization phenomenon was observed. As previously explained, the main challenge was to conserve the original size distribution of the powders. The results showed that only few stable and hard agglomerates larger than 1 mm were formed, representing less than 10% of the bed weight. Before granulometric measurements, those "big" agglomerates were separated easily by sieving. Figure 2(a) shows that the volume size distributions remained quite unchanged after CVD despite a small peak detected in the 1 – 10 µm range, showing that some micronic hard agglomerates remained after sieving. Figure 2(b) presents size distributions in particles number. The hard agglomerates are not visible anymore indicating that they represent a very small proportion of the total mass of powders.

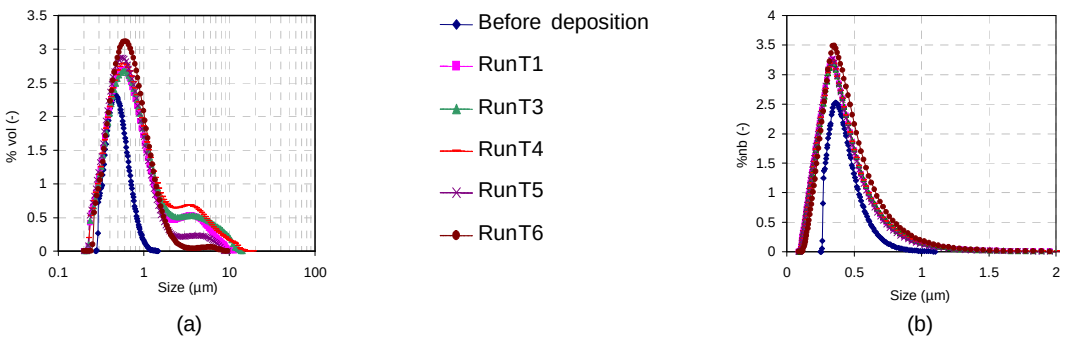

(a) (b)

Figure 2: Size distribution of uncoated and Si-coated TiO_2 powders measured by laser granulometer. a) volumetric percentages, b) total number of particles percentages.

Figure 3(a) presents the results obtained by Raman spectroscopy. The spectrum obtained before silicon deposition, exhibits four peaks at 144, 398, 516 and 639 cm^{-1} characteristic of anatase phase of TiO_2 [18]. After CVD, the Raman spectrum is different. The peak at 612 cm^{-1} can be attributed to rutile phase of TiO_2 and the peaks at 154 cm^{-1} and 400 cm^{-1} are attributed, respectively to the anatase and rutile phase, although they are broadened and shifted relative to the corresponding features in bulk TiO_2 [18, 19]. It has been demonstrated [20] that these shifting and broadening could be related to some oxygen vacancies, maybe due to a partial reduction of the material. A new peak appeared at 500 cm^{-1} characteristic of the presence of amorphous silicon [21].

Figures 3(b) and 3(c) present TEM views of TiO_2 particles before and after CVD for run T7. In Figure 3(b) grains appear aggregated due to interparticles cohesive forces. In Figure 3(c) blobs of amorphous silicon can be observed and the film does not seem to be fully continuous. For this particle, the film thickness is approximately 10 nm which is in good agreement with the calculated value of Table 2.

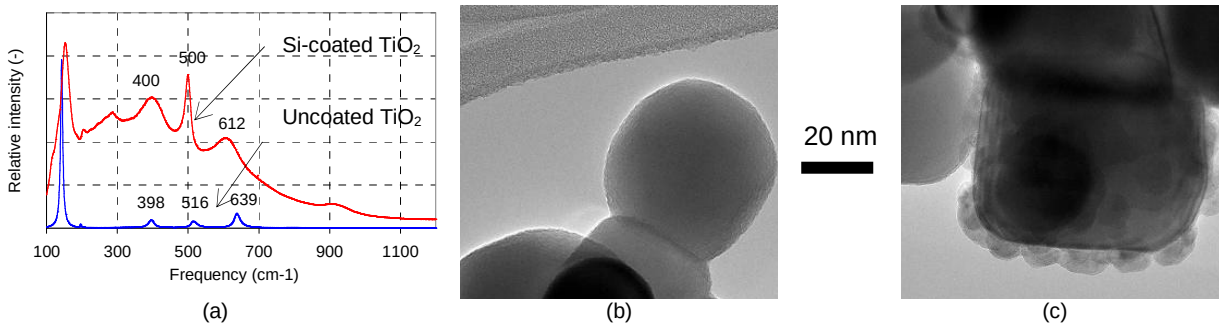

(a) (b) (c)

Figure 3: (a) Raman spectra for uncoated and Si-coated TiO_2 powders (run T3); TEM images of TiO_2 powders (b) before silicon deposition; (c) after silicon deposition for run T7.

FBCVD OF SILICON ON ALUMINA POWDERS OF 342 MICRONS

Experimental study

The operating conditions tested and the corresponding results are listed in Table 3. The inlet volumetric percentage of silane in nitrogen has been varied between 0.5 to 10.

Run	Temperatures (℃)		U/Umf	Initial weight of powders (g)	Ho/D	Weight of injected Si (g)	Run duration (min)	Weight of deposited silicon (g)	Silane conversion rate (%)	Calculated thickness of deposited Si (microns)
	Distributor	Top of the bed								
A1	575	640	4.2	800	4	6.74	21.5	5	74.18	0.6
A2	605	630	4.4	800	4	7.14	21.5	5.9	82.7	0.73
A3	580	660	4.6	800	4	25.1	21	17.8	70.9	2.1
A4	550	620	4.2	800	4	24	21	17.5	72.9	2
A5	570	615	4.2	800	4	20.3	25	16.4	80.9	1.95
A6	550	570	4	400	2	5.5	22	3.6	65.3	0.87
A7	560	610	4.5	800	4	30.9	21	24.2	78.3	2.9
A8	515	530	4.28	400	2	21.9	13	3.2	14.6	0.78
A9	520	535	5	600	3	38.8	22	6.6	17	1
A10	550	580	4	800	4	40.7	40	24.2	59.4	2.7
A11	550	580	4.1	800	4	41	40	24.4	59.5	2.7
A12	552	576	4.1	1300	6.5	41.4	40	36.3	87.7	2.5

Table 3: Operating conditions and experimental results for silicon deposition on Al_2O_3 powders of Geldart's group B.

First, the reproducibility of the results has been verified through runs A10 and A11. Thermal gradients are still present for these runs but they can be lowered to around 15-20℃ for the lowest temperatures tested, which gave acceptable uniformity of deposition primarily due to the intense circulation of the particles inside the bed. The reason to increase the initial FB weight (run A12) is to decrease this gradient by taking advantage of better thermal transfers between the reactor walls and powders.

The deposition rate varies between 30 to 120 nm/min. As previously observed in the literature [16,17,22], this parameter and the silane conversion increase with temperature. The silane conversion logically increases with the initial FB weight (runs A6 and A12). For runs A3 to A5 and A7 to A12, the weights of injected silicon are high. For these runs, some reversible disturbances of the thermal profile and pressure drop along the FB have been observed. They are due to a partial de-fluidisation of the bed, probably related to the appearance of short-lived agglomerates; indeed silicon dangling bonds are probably formed on the surface of each particle during deposition, acting as glue for the surrounding particles [16]. Such disturbances have not been observed for TiO_2 particles because of the low amount of SiH_4 used.

For the conditions tested, the size distribution of the powders has not been modified by deposition. SEM analyses revealed that deposition seems uniform on powders and that for the highest weights of silicon injected, coating thickness of several hundreds of nanometers was achieved. Some Raman and XRD measurements have shown that when the FB temperature was lower than 610°C, silicon deposition was mainly amorphous whereas it was polycrystalline at higher temperature.

CFD modelling of the process

The CFD open-source code MFIX [23], a benchmark tool for the simulation of FB, was used for this study. 2-D axisymmetric and 3-D calculations were performed using the continuum model, the drag law of Syamlal-O'Brien [24], kinetic theory of granular materials with an algebraic form for granular temperature equation for the solid phase stress tensor in the viscous regime and the Schaeffer model [25] for the calculation of the solid phase stress tensor in the plastic regime. Concerning the alumina powder, a mean Sauter diameter of 330 µm and an internal angle of friction of 40° were considered. The latter value corresponds to the repose angle (note that for non-cohesive powders, these two parameters are identical [26]). Since we did not find any data in the literature about the coefficient of restitution for the collisions of alumina particles, the default value of 0.8 was used.

Some preliminary calculations showed that using the Superbee method for spatial discretization scheme (order 2), the grid independent results were achieved by using 200 cells along the axial direction for a height of 0.4 m, 15 cells along the radial direction for the half diameter, and for 3-D calculations, 6 angular cells. This result is true over all the range of the operating conditions studied.

As a first step only the pure hydrodynamic behaviour of the bed has been modelled. In this study, experiments were performed using 800 g of powder fluidized with air at ambient temperature in the glass column, using average superficial gas velocities, U_g, between 5 and 40 cm/s. The fluidization plateau was reached at a minimum fluidization velocity (U_{mf}) of about 12.5 cm/s, the pressure drop across the bed being very close to the theoretical value of 4000 Pa. Then, the bed behaviour was more specifically studied for 3 gas velocities: 18, 25 and 30 cm/s, using the video camera. This allowed determining accurately minimum and maximum average heights of the fluctuating bed for each gas velocity.

The knowledge of U_{mf} allowed adjusting the coefficients of the Syamlal-O'Brien drag correlation [24]. Then, 2-D axisymmetric and 3-D MFIX simulations were performed for the 3 gas velocities studied. Values of minimum, maximum and average bed expansions, H/H_{mf}, obtained from experiments and from calculations are compared in Figure 4. All calculations overestimate bed expansions and fluctuations but results obtained with 3-D simulations are much closer to experimental data than results obtained with 2-D calculations. It appears that the best prediction of 3-D calculations is obtained for the highest velocity (U_g=30 cm/s) with overestimations of average bed heights and fluctuations of about 7%. Note that this gas velocity was used for experiments of Si CVD.

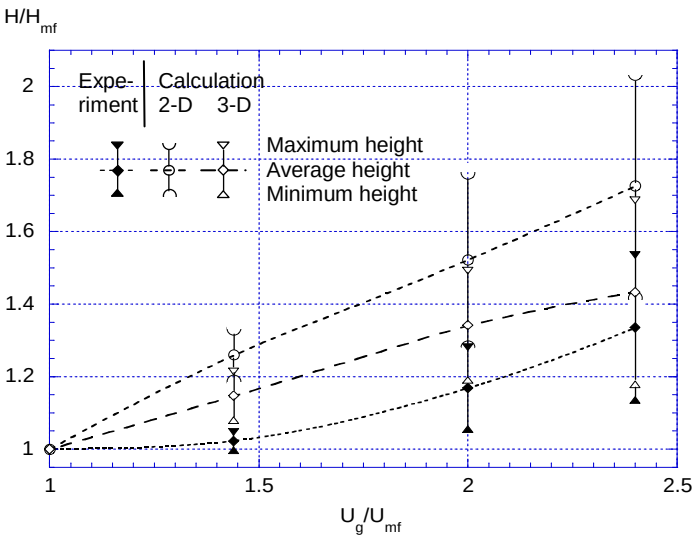

Figure 4: Minimum, maximum and average bed expansions *vs.* relative gas velocity obtained from experiments and from 2-D and 3-D calculations

The second step aimed at modelling the silicon deposition process. First, thermal profiles existing along the FB and the presence of the tube of 6 mm in diameter along the column axis were included in the simulation. A chemical model was then implemented in MFIX to simulate the deposition of silicon from SiH_4. The kinetic law of Furusawa *et al.* [27] was chosen because it is one of the sole established for the FBCVD process for our conditions. In the present version of the model, only the overall reaction of silicon deposition from silane is considered, leading to the production of gaseous hydrogen:

$$SiH_4 \rightarrow Si + 2H_2$$

Runs A5 and A7 of Table 3 were then simulated in 3-D with an average bed temperature of 600℃, an increase of the axial temperature during deposition of about 50℃ measured along the bed, the fluidization ratio being close to 4.5.

The coefficients of the Syamlal-O'Brien drag correlation have been adjusted considering a value of U_{mf} equal to 7.5 cm/s at 600℃. Note that a preliminary modelling study showed that discrepancies of about 10% on bed expansions and fluctuations had no effect on the final conversion rates of silane calculated.

Instantaneous fields of void fraction and normalized silane mass fraction calculated after 7.1 s of deposition for run A7 are presented in Figure 5. Figure 5(a) shows that a slug of gas is present on about 60% of the FB height due to the high H_0/D ratio used. Some millimetre scale bubbles of gas are present near the distributor but the bed is clearly in the slugging regime. Although Figure 5(b) shows complete conversion of silane in the exit gas, the average conversion is indeed much less than 100%. Note the low conversion in the gas at the center of the slug. When the slug erupts at the top, gases with low silane conversion will exit the reactor. The average silane conversion was found by time-averaging the instantaneous values.

Final conversion rates of silane measured and calculated for run A5 are of 81% and 79% respectively. For run A7, they are of 78% and 65% respectively. This agreement is quite good considering that only the heterogeneous phase reaction kinetics have been implemented in the model.

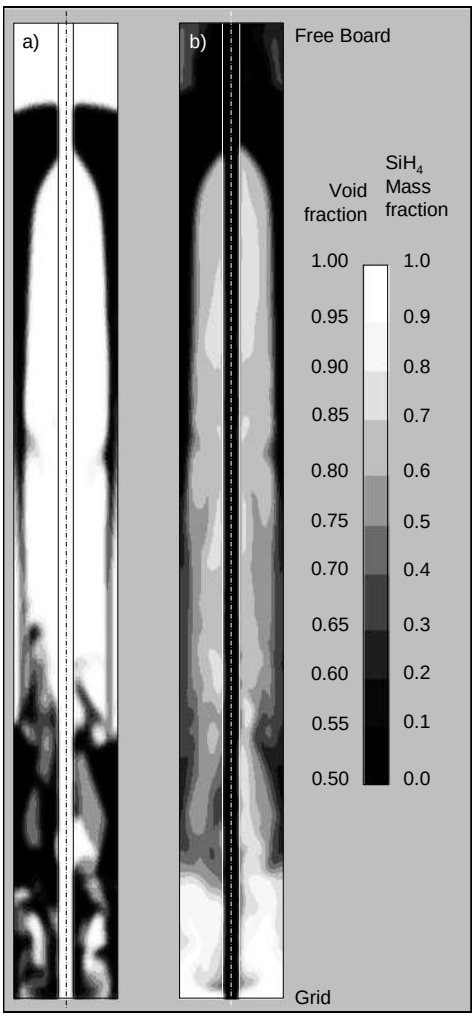

Figure 5 : Void fraction (a) and silane mass fraction (b) calculated after t=7.1 s for run A7

CONCLUSION

The first results of silicon deposition by vibro FBCVD on TiO_2 submicron powders show that the original granulometry is preserved for all the particles except for those present where fresh silane enters. In order to limit this phenomenon, new experiments are under progress, in particular using a sequential feeding of silane. CFD simulations of both FB hydrodynamics and of reactive mass transfers existing during silicon CVD are in good agreement with the experimental data. Our future work is to implement (i) the homogeneous reactions occurring during silane pyrolysis, (ii) the column vibrations and (iii) extend this code to represent beds of cohesive particles, to better understand the physical and chemical phenomena involved when treating submicron powders.

Acknowledgements: The MFIX simulations have been performed on the GridMip platform of the French Grid'5000 network.

REFERENCES

[1] Geldart D., ''Types of gas fluidization'', Powder Technology, 7, 285-292 (1973).
[2] Hakim L. F., Portman J. L., Casper M. D., Weimer A. W., ''Aggregation behavior of nanoparticles in fluidized beds'', Powder Tech., 160, 149-160 (2005).
[3] Kuipers N.J.M., "Fluidization of a bed of cohesive powder", US. Patent: WO 95/15213 (1995).
[4] Dutta A., Dullea L.V., "Effect of external vibration and addition of the fibres on the fluidization of a fine powder", AIChE Symp. Ser. 93, 38–47 (1994).
[5] Kim Jimin, Han Gui Young, ''Effect of agitation on fluidization characteristics of fine particles in a fluidized bed'', Powder Tech., 166(3), 113-122 (2006).
[6] Alavi S., Caussat B., ''Experimental study on fluidization of micronic powders'', Powder Tech., 157, 114-120 (2005).
[7] Xu C., Zhu J., ''Parametric study of fine particle fluidization under mechanical vibration'', Powder Tech., 161, 135-144 (2006).
[8] Van Wachem B., Schouten J.C., Van den Bleek C.M., Krishna R., Sinclair J.L., "Comparative analysis of CFD models of dense gas-solid systems", AIChE J., Vol. 47, No. 5, 1035-1051 (2001).
[9] Goldschmidt M. J. V., Kuipers J. A. M. and van Swaaij W. P. M., "Hydrodynamic modelling of dense gas-fluidised beds using the kinetic theory of granular flow: effect of coefficient of restitution on bed dynamics", Chem. Eng. Sci., 56(2), 571-578 (2001).
[10] Taghipour F., Ellis N. and Wong C., "Experimental and computational study of gas–solid fluidized bed hydrodynamics", Chem. Eng. Sci., 60(24), 6857-6867 (2005).
[11] Johansson K., Van Wachem B.G.M. and Almstedt A.E., "Experimental validation of CFD models for fluidized beds: Influence of particle stress models, gas phase compressibility and air inflow models", Chem. Eng. Sci., 61(5), 1705-1717 (2006).
[12] D. Gidaspow, L. Huilin, "Equation of state and radial distribution functions of FCC particles in a CFB," AIChE Journal, 44(2), 279 – 293 (1998).
[13] Weber M., "Simulation of Cohesive Particle Flows in Granular and Gas-Solid Systems", Ph. D. Thesis University of Colorado (2004).
[14] Guenther C., O'Brien T., Syamlal M., "Fourth International Conference on Multiphase Flow", New Orleans, LA, pp. 1–12 (2001).
[15] Carr R., ''Evaluating flow properties of solids'', Chem. Eng., 18, 163-168 (1965).
[16] Caussat B., Hemati M., Couderc J.P., ''Silicon deposition from silane or disilane in a fluidized bed -Part I : Experimental study'', Chem. Eng. Sci., 50(22) 3615-3624 (1995).
[17] Tejero-Ezpeleta M. P., Buchholz S., Mleczko L., ''Optimization of Reaction Conditions in a Fluidized-Bed for Silane Pyrolysis'', Can. J. Chem. Eng., 82(3), 520-529 (2004).
[18] U. Balachandran and N. G. Eror, Raman spectra of titanium dioxide, J. Solid State Chem., 42(3), 276-282 (1982).
[19] S. P. S. Porto, P. A. Fleury, and T. C. Damen, Raman Spectra of TiO_2, MgF_2, ZnF_2, FeF_2, and MnF_2**,** Physical Review 154 (2), 522-526 (1967).
[20] J.C.Parker and R.W. Siegel, Raman microprobe study of nanophase TiO_2 and oxidation-induced spectral changes, J.Mater. Res, 5(6),1246-1252 (1990).
[21]A. Zwick et R. Carles, multiple order Raman scattering in crystalline and amorphous silicon, Phys. Rev. B, 48(9), 6024 (1993).
[22] Kojima T., Morisawa O., ''Optimum process conditions for stable and effective production of a fluidized bed CVD reactor for polycrystalline silicon production'', Proceedings of the 8th European Conf. on CVD, Glasgow, Scotland, Hitchman et Archer ed., C2-475 (1991).
[23] www.mfix.org.
[24] Syamlal, M., and T.J., O'Brien, "Fluid dynamic simulation of O3 decomposition in a bubbling fluidized bed," AIChE J., 49, 2793-2801 (2003).
[25] Schaeffer D.G., "Instability in the Evolution Equations Describing Incompressible Granular Flow", J. Diff. Eq., 66, 19-50 (1987).
[26] Terzaghi K., "Theoretical Soil Mechanics", Wiley, New York, NY, (1942).
[27] Furusawa T., Kojima T. and Hiroha H., "Chemical Vapor Deposition and Homogeneous Nucleation in Monosilane Pyrolysis Within Interparticle Spaces – Application of Fines Formation Analysis to Fluidized Bed CVD", Chem. Eng. Sci., 43-8, 2037-2042 (1988).